ACS APPLIED MATERIALS & INTERFACES

Research Article

www.acsami.org

Special Reactive Oxygen Species Generation by a Highly Photostable BODIPY-Based Photosensitizer for Selective Photodynamic Therapy

Yen-Chih Lai,[†] Sheng-Yuan Su,[‡] and Cheng-Chung Chang*[,†]

[†]Graduate Institute of Biomedical Engineering, National Chung Hsing University, 250 Kuo Kuang Road, Taichung, 402, Taiwan, R.O.C.

[‡]Department of Chemistry, National Chung Hsing University 250, Kuo Kuang Road, Taichung 402, Taiwan, R.O.C.

Supporting Information

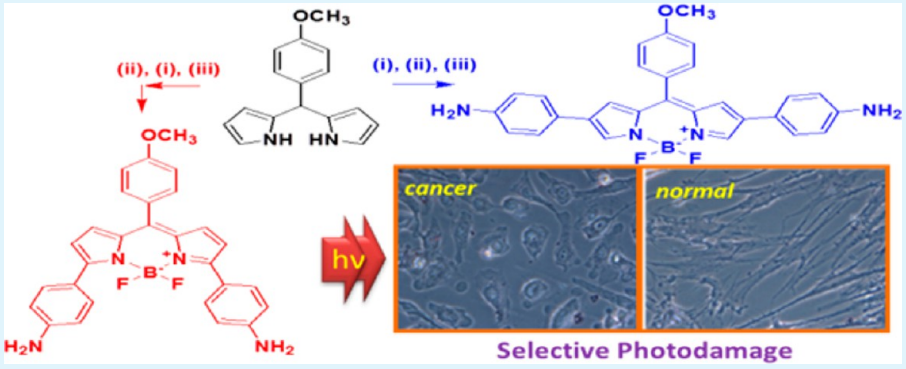

ABSTRACT: We introduce a new class of photostable, efficient photosensitizers based on boron-dipyrromethene (BODIPY) derivatives that can generate singlet oxygen and super oxide simultaneously under irradiation. For compound preparation, appropriate regulation of the reaction conditions and control of specifically substituted BODIPY derivatives have been achieved. After biologically evaluating the intracellular uptake, localization, and phototoxicity of the compounds, we conclude that 3,5-dianiline-substituted BODIPY is a potentially selective photodynamic therapy candidate because its photodamage is more efficient in cancer cells than in normal cells, without apparent dark toxicity. Furthermore, direct comparison of photodamage efficacy revealed that our compound has better efficacy than Foscan and nearly equal efficacy to that of methylene blue.

KEYWORDS: *photosensitizers, photostability, photodynamic therapy, reactive oxygen species, tumor selectivity, boron-dipyrromethene*

1. INTRODUCTION

Photosensitizers, light and oxygen are all necessary elements for photodynamic therapy (PDT) to execute a series of photochemical reactions that frequently generate reactive oxygen species (ROS) from the photosensitizer and then cause tissue damage in the regions where these three key components remain.[1] There are many reported or commercially available photosensitizers; the most well-known clinically relevant PDT agents are cyclic tetrapyrroles (e.g., porphyrins, chlorins, and bacteriochlorins).[2,3] In addition, phenothiazinium-based structures are another well-known category of this type of PDT agent.[4,5] By comparison, cyclic tetrapyrroles are more complicated to synthesize and modify, whereas phenothiazinium-based structures can be made more easily but present low light-to-dark toxicity ratios.[6] That is, most photosensitizers present a low photostability, structural instability, or usable limit under certain solvents,[1,7,8] which confines their application. Thus, developing a new generation of photosensitizers with high efficiency and photostability that are widely applicable under various conditions is important.

Selective photodamage is the most important criterion for a superior PDT reagent. In the clinic, photosensitizer delivery is performed through a traditional approach by controlling the time discrimination between photosensitizer injection and light irradiation.[9] This approach lacks a targeting policy, causes poor tumor selectivity, and leads to a low tumor/normal tissue accumulation ratio.[10] The delivery efficiency to cancer cells and subcellular distribution of a photosensitizer usually depend on cellular processes as well as the structural characteristics of the molecule itself.[11] Therefore, to improve the selective delivery of a photosensitizer to tumor tissue, the literature reports that this photoactive compound can be conjugated to hydrophilic polymers,[12] carbohydrates,[13] carrier proteins,[14] oligonucleotides,[15] epidermal growth factor,[16] and antibodies.[17] However, most of these high-molecular-weight complexes are difficult to synthesize and purify and are usually located in the cytoplasm or cytoplasmic membranes rather than in photosensitive intracellular organs, such as mitochondria, endoplasmic reticulum (ER), and nucleus.

Received: August 26, 2013
Accepted: December 6, 2013
Published: December 6, 2013

BODIPY (boron-dipyrromethene) derivatives provide high absorption extinction coefficients, sharp fluorescence emissions with high fluorescence quantum yields, photostability, and low sensitivity to environmental variation.[18,19] Thus, BODIPY derivatives have attracted much research interest and have been used in laser dyes,[20] labeling reagents for markers,[18−22] fluorescent switches for chemosensors,[23−27] energy transfer for cassettes,[28] and harvesting arrays for solar cells.[29,30] The novel application of BODIPY derivatives in photosensitization was achieved by attaching a functional group that donates electrons to stabilize the photoexcited BODIPY core and to quench fluorescence, thereby promoting a triplet-state lifetime.[31] Specifically, heavy atoms are incorporated into the structure as a strategy to facilitate intersystem crossing and to promote the singlet oxygen yield to become a new generational candidate for photodynamic sensitizers.[32−35] This class of molecules appears to satisfy the required criteria of a good photosensitizer (high singlet oxygen yield, photostability, and long-wavelength absorption); however, a photosensitizer must be dark-nontoxic to be a PDT candidate, and these molecules are not.[36] More importantly, on the basis of the above considerations, it is rare to find BODIPY-based photosensitizers that offer selective photodamage to cancer cells but not to normal cells or tissues. Hence, it is possible to design and produce a new generation of BODIPY-based photosensitizers that can meet the requirements of dark-toxicity and non-selective photodamage without losing their unique optical characteristics by appropriate chemical modification. This strategy can be easily achieved by attaching aryl groups directly to the BODIPY core, which can be constructed from inexpensive pyrroles but not from dimethyl pyrroles. In this study, by controlling the bromination sequence, the synthesis of 3,5- or 2,6-diaryl-substituted BODIPY derivatives gives a good yield. Preliminary biological studies on one of these dyes indicated that this type of compound is highly membrane permeable and that it can selectively localize within specific subcellular organelles, suggesting promising PDT applications for these molecules. Consequently, we present a novel photosensitizer, 3,5-diaryl-substituted BODIPY, that is highly efficient and photostable; more importantly, it showed selective PDT behavior.

2. EXPERIMENTAL SECTION

2.1. Materials. Generally, the chemicals employed in this study were of the best grade available and were obtained from Acros/Aldrich Chemical Co. or Merck Ltd. and used without further purification. All of the solvents for spectral measurements were of spectrometric grade.

2.2. Apparatus. The absorption and fluorescence spectra were generated using a Thermo Genesys 6 UV−vis spectrophotometer and a HORIBA Jobin-Yvon Fluoromas-4 spectrofluorometer, respectively. The cellular fluorescence images and dual-staining fluorescence images were obtained using a Leica AF6000 fluorescence microscope with a DFC310 FX digital color camera and a Leica TCS SP5 confocal fluorescence microscope. The light source used for the measurements of the singlet oxygen yield and PDT cell death was an Asahi Spectra Full spectrum Xenon light source Lax-Cute.

2.3. Cell Culture Conditions and Compound Incubation. The human lung adenocarcinoma cell line A549 was maintained in RPMI-1640 medium containing 1% penicillin/streptomycin, 2.0 g/L of sodium bicarbonate, and 10% fetal bovine serum FBS. MRC-5 normal human embryonic lung fibroblast cells and HeLa human cervical cancer cells were maintained in modified Eagle's medium (MEM) containing nonessential amino acids, Earle's salts, L-glutamine, 1 mM sodium bicarbonate, 1 mM sodium pyruvate, 1% penicillin/streptomycin, and 10% FBS. The cells were cultured at 37 °C in a humidified atmosphere (95% air and 5% CO_2) and were then seeded onto coverslips and incubated for 24 h before the observation of cellular localization. On the next day, cells were incubated with different concentrations of compounds for 12 h; the DMSO stock solutions of the compounds were diluted in serum-free medium before use (1:100 v/v).

2.4. Light-Induced Cytotoxicity Assay. Three different cell types were examined in the assay: MRC-5 normal human lung cells, A549 lung cancer cells, and HeLa human cervical cancer cells. Varying concentrations of compounds were incubated with the cells in the dark for 12 h. Subsequently, the culture medium was removed, and fresh culture medium was then added to each well. The plates were irradiated using a light source and incubated for a further 24 h at 37 °C. All assays were carried out in three individual runs, and the average result is presented. Methylene blue and Foscan were used as comparative standard controls and were assayed according to previously documented procedures.[37]

2.5. Extraction and Quantification of Compounds in Cells. HeLa cells were seeded into 60 × 15 mm^2 cell culture dishes. A compound was added to one dish when the cells reached ∼90% confluence, and the cells were incubated for 12 h. After incubation, all dishes were washed with PBS, and the cells were removed from the substrate with trypsin and pelleted. Ethyl acetate (1.8 mL) was added to extract the compound after the collected cells (2×10^6) were sonicated for 1 h. Both absorbance and fluorescence signals in the organic phase were recorded. A similar protocol was also applied to extract the compound and to obtain the spectral signal measurement of MRC-5 normal cells (the cell number in collected suspension was consistent with that of cancer cells, 2×10^6).

2.6. Measurement. The experimental conditions for singlet oxygen yield and PDT cell death measurements were as previously described.[38] A full-spectrum Xenon lamp passes through a 400−700 nm mirror module, and the light was then filtered with a 510 nm long-pass (lp) filter before exiting the optional light guide and collimator lens (the light power was 6 mW/cm^2 on the dish surface). The singlet oxygen quantum yield of a compound in organic solvent was determined by a photo-steady-state method using 1,3-diphenylisobenzofuran (DPBF) as the scavenger. The singlet oxygen quantum yield from compounds in D_2O was calculated using a phosphorescence detection method. A HORIBA Jobin-Yvon Fluoromas-4 spectrofluorometer (coupled with an InGaAs LN_2 DSS detector, 1427B) at 650 nm was used as the excitation source, and the radiation emitted at 1270 nm was directly detected. Four different concentrations of compounds in D_2O were tested. The absorbance of the sample and standard (methylene blue) were kept the same. Quantum yield values were calculated by comparing the emission of samples and standards. The superoxide generation from compounds that were in aqueous solution was determined by a photo-steady-state method using 4-((9-acridinecarbonyl)amino)-2,2,6,6-tetramethylpiperidin-1-oxyl (TEMPO-9-ac, Invitrogen, Carlsbad, CA) as the radical detector. Dual staining of the tracker and the compound was performed as follows: the cells were incubated with a compound for 12 h and then treated with organelle probes (5 μM, Mito Tracker green FM for 20 min at 37 °C, ER Tracker green for 30 min at 37 °C) followed by washing with PBS before observation. The excitation sources were a green light that was guided through a 535 ± 25 nm band-pass filter, with emission collected through a 590 nm long-pass filter (red emission of compound), and a blue light cube in which light passed through a 470 ± 20 nm bp filter, with emission collected through a 510 nm lp filter to collect the green emission of the probes. Once the definite yellow color image was presented, the compound was considered to have colocalized with the probes. PDT-induced phototoxicity was evaluated using a Hoechst 33342 (H-1399, Invitrogen, USA) and propidium iodide (PI, P3566, Invitrogen, USA) staining assay visualized under a fluorescence microscope. To avoid the possible interference from the probes, the probes were stained after PDT performance was tested.

Scheme 1. Synthetic Route to BODIPY-Based Photosensitizers 2,6DAN and 3,5DAN[a]

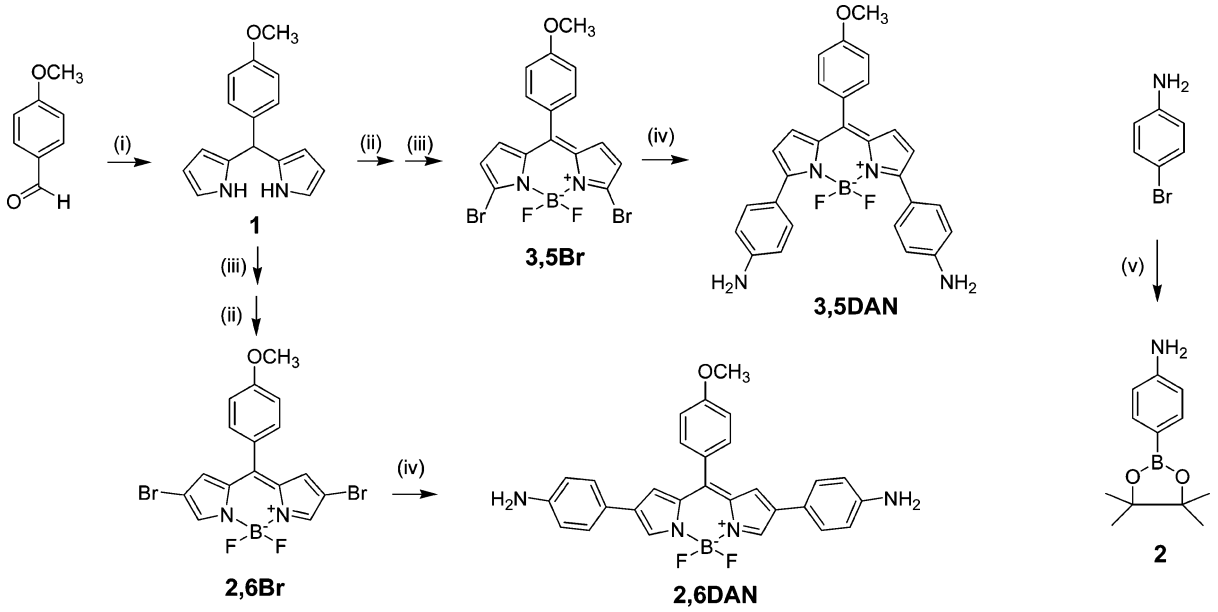

[a]Reagents and conditions: (i) pyrrole, TFA, rt; (ii) NBS, THF, ice bath; (iii) DDQ, THF, rt then Et_3N/BF_3OEt_2, toluene, reflux; (iv) K_2CO_3, $(o\text{-tol})_3P$, $Pd(OAc)_2$, DME/H_2O 5:1, compound 2, reflux; (v) $Pd(PPh_3)_2Cl_2$, pinacolborane, dioxane/Et_3N, reflux.

3. RESULTS AND DISCUSSION

3.1. Molecular Preparation and Basic Spectroscopic Property. BODIPY derivatives 2,6DAN and 3,5DAN were synthesized by the different routes outlined in Scheme 1. Bromination is the key reaction for molecule preparation in this study. 8-(4-Methoxyphenyl)boron-dipyrromethane, an intermediate precursor of compound 2,6Br, was obtained upon $BF_3\cdot Et_2O$ complexation of compound 1. Then, 2,6-dibromo-substituted BODIPY was prepared by treating 1 equiv of 8-(4-methoxyphenyl)boron-dipyrromethane with 2.2 equiv of *N*-bromosuccinimide (NBS). Alternatively, when compound 1 was brominated with NBS first, the main product was 3,5-dibromo-substituted dipyrromethane, which is unstable because it is easily protonated, especially in the column flushing purification process. Therefore, we prepared compound 3,5Br in a sequence of steps in a one-pot reaction directly from compound 1. Notably, the use of 2.2 equiv of NBS provided dibromo-BODIPY in good yield along with a minor amount of monosubstituted bromine. Here, even with an excess amount of the brominating agent, no regioisomeric products, such as 3,5-dibromo-substituted product in 2,6Br or 2,6-dibromo-substituted product in 3,5Br, were detected in the reaction. Additionally, in the last step, both 2,6Br and 3,5Br were coupled with compound 2 with similar yield under the same reaction conditions.

In this investigation, the BODIPY moiety was selected as the electron acceptor, and aniline was chosen as the electron-donating unit. When comparing the spectra properties of these chromophores, as shown in Figure 1, 2,6-disubstituted product 2,6DAN showed no significant solvent polarity dependence and a lower transition energy in all investigated solvents, with broader peak patterns in the absorption spectra. Meanwhile, higher extinction coefficient values but low quantum yields were obtained. This finding indicates that in the ground states these chromophores were significantly stabilized by solvation and that the auxiliary electron-donating ability of aniline units offered better effective conjugation to the BODIPY core.

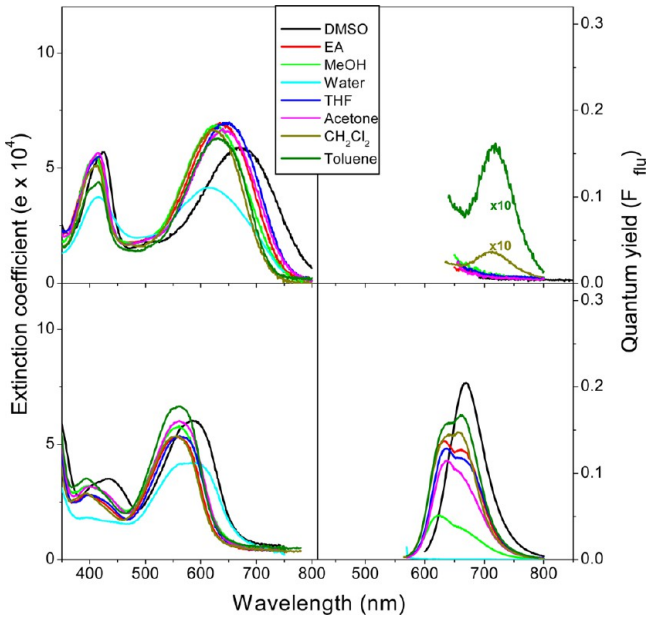

Figure 1. Absorption (left, represented by extinction coefficient) and emission (right, represented by quantum yield) spectra of compounds 2,6DAN (top) and 3,5DAN (bottom) in different solvents. Excited wavelengths are absorption maxima. Determination of quantum yields is relative to rhodamine B (Φ = 0.69).[39]

However, 3,5-disubstituted product 3,5DAN also showed no significant solvent polarity dependence, but luminescence quantum yields were increased to 0.2 in organic solvents. These results suggested a strong push−pull effect, which was caused by electron transfer from the aniline donor to the BODIPY acceptor in the 3,5-disubstituted product compound. However, we expect that this type of fluorophore will be able to penetrate cell membranes, and its unique optical properties can be checked in cell lines.

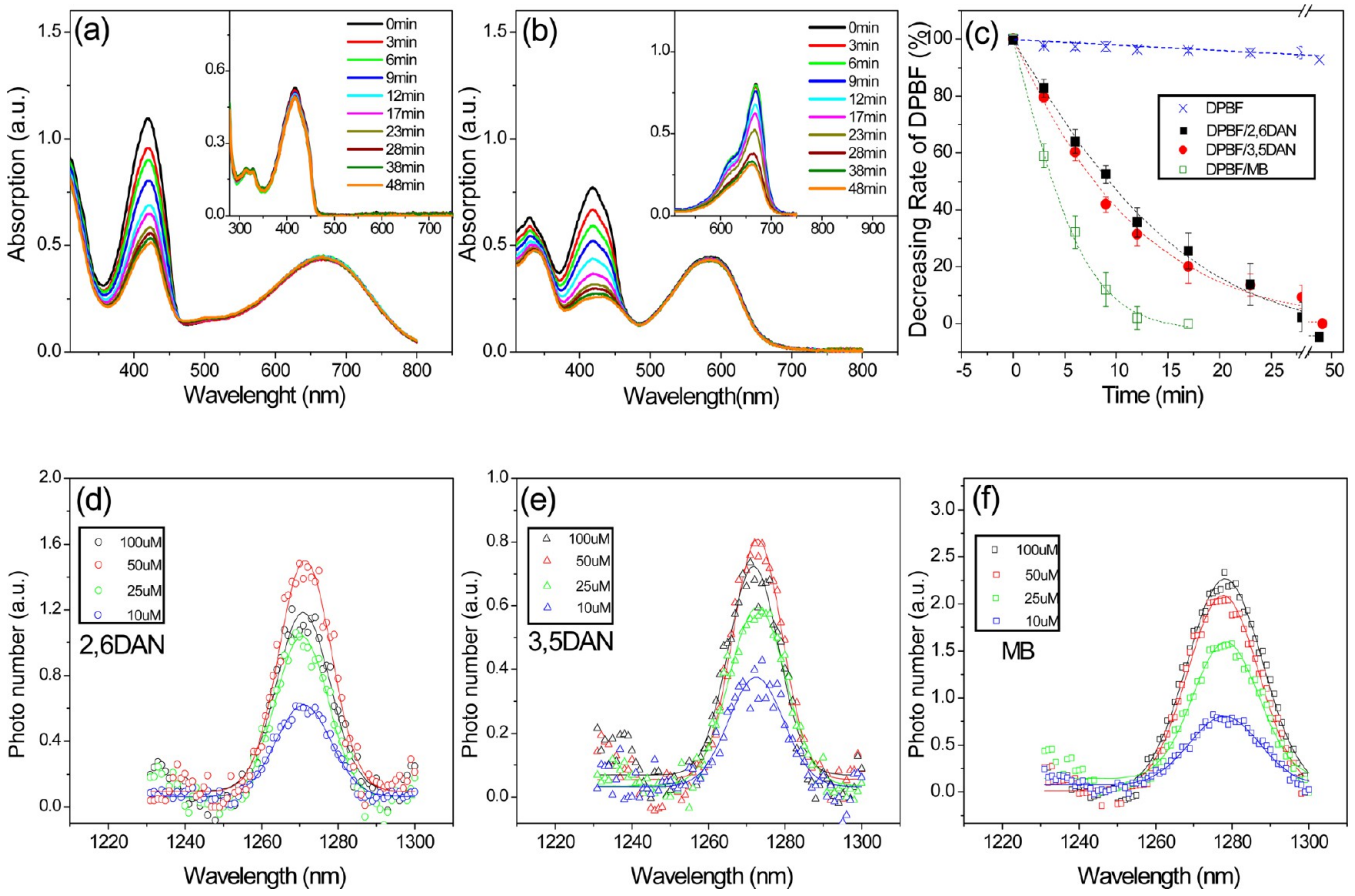

Figure 2. Absorption spectra variations of 20 μM DPBF consumption in the presence of 10 μM (a) 2,6DAN and (b) 3,5DAN in DMSO after irradiation with an average 6 mW/cm^2 light source through the 510 nm long-pass filter. (c) Relative DPBF oxidation rates by singlet oxygen in which each data point represents the average of three separate experiments. The inset in panel a is control DPBF without adding a compound, and the inset in panel b is with methylene blue under the same experimental conditions. (d–f) Near-infrared luminescence of singlet oxygen (~1270 nm) sensitized by 650 nm irradiation of different concentrations of compounds in D_2O.

3.2. Singlet Oxygen Generation and Photostability. Singlet oxygen production was monitored using the known singlet oxygen acceptor 1,3-diphenylisobenzofuran (DPBF)[40] and by following the disappearance of the 410 nm absorbance band of DPBF at an initial concentration of 20 μM (2 times the concentration of the compound). The rates of DPBF oxidation by these two compounds in DMSO solvent were investigated with an visible-light source (400–700 nm with a 510 nm long-pass filter) for the irradiation period (Figure 2a–c). Compounds 2,6DAN and 3,5DAN both presented similar DPBF oxidation-rate curves, and their singlet oxygen yields were estimated to be about one-third of that of methylene blue (MB). A similar experiment was performed in toluene solvent, and we observed higher singlet oxygen yields equal to MB, as shown in Figure S1. The solvent-dependent quantum yield of singlet oxygen was also found in another BODIPY system.[41] Thus, the singlet oxygen emission signal at 1270 nm in D_2O was directly measured to calculate the actual the singlet oxygen quantum yield (Φ_Δ). Figure 2d–f shows the concentration dependence of the signals for compounds 2,6DAN, 3,5DAN, and MB. Here, we found that the optimum concentration for measurement is 50 μM for 2,6DAN and 3,5DAN, and the Φ_Δ values were obtained as 0.38 and 0.40 by the relative method using methylene blue as the reference (Φ_Δ = 0.52 in D_2O).[42] Additionally, the inset in Figure 2b shows that under this irradiation condition the photostabilities of these two compounds were better than that of methylene blue (MB). Good photostability upon repetitive excitation is regarded as highly desirable in PDT applications because photobleaching of photosensitizers usually produces photodegradation side products that may lower the efficiency of ROS generation. Moreover, when a photosensitizer is used as a tumor-visualizing tool in PDT, high photostability is required to allow for tracing over a long observation period.[43]

However, the singlet oxygen levels apparently increased when the system was irradiated using a white light source under the same irradiation power (400–700 nm, no filter, 6 mW/cm^2 on the dish surface, Figure S2). This finding indicates that the S_0–S_2 transition absorption bands of the compound at approximately 400 nm contributed to some singlet oxygen yield. However, photodegradation was observed in compound 2,6DAN because the absorption of 2,6DAN decreased during the irradiation period, but that of 3,5DAN remained unchanged. This result indicated that the S_0–S_2 transition energy of the compound supported the extra singlet oxygen yield but also caused some degree of degradation to the compound itself. The photodegradation of 2,6DAN is speculated to be due to the substituted groups of BODIPY, which more easily rotate in the 2,6 position than in the 3,5 position. Moreover, the NMR results revealed that the proton chemical shifts of the NH_2 of aniline in 2,6DAN is downfield from that of 3,5DAN. This means that photoinduced proton

transfer (loss) may occur more easily in 2,6DAN, especially under higher irradiating energy. Nevertheless, all of these results emphasize that 3,5DAN is highly photostable in visible-light applications.

3.3. Real-Time Photodamage and Photostability in Cells. Once these two compounds were shown to be photostable and able to generate singlet oxygen, we examined whether the compounds could be used as a tool for cell photosensitization. Figure 3 illustrates the photodamage process from a real-time video recorded under a fluorescence microscope with a color CCD that measured fluorescence using a 535 ± 25 nm band-pass filter as an excitation light source and a red filter for emission collection (590 nm long pass). Plasma membrane bleb formation and acute cell death caused by illumination with green light were clearly observed in compound-treated cells. Irradiation-time-dependent fluorescent images show nearly constant emission intensities, which further confirms the photostability behavior observed in Figure 2. Furthermore, these two compounds both caused apparent photodamage to cancer cells, but only compound 2,6DAN caused apparent damage to normal cells. This important result indicated that 3,5-disubstituted BODIPY (3,5DAN), but not 2,6-disubstituted BODIPY (2,6DAN), may be a selective PDT candidate. Fluorophores that emit in the red wavelength range are extremely valuable in biological microscopy because they minimize cellular autofluorescence and increase flexibility in multicolor experiments. Our result suggests that because of its selective photodamage, high photostability, high extinction, and apparent red emission signal in cells 3,5DAN is a potentially useful reagent for use as a tracing marker and the study of oxidative stress for cell photosensitization or PDT.

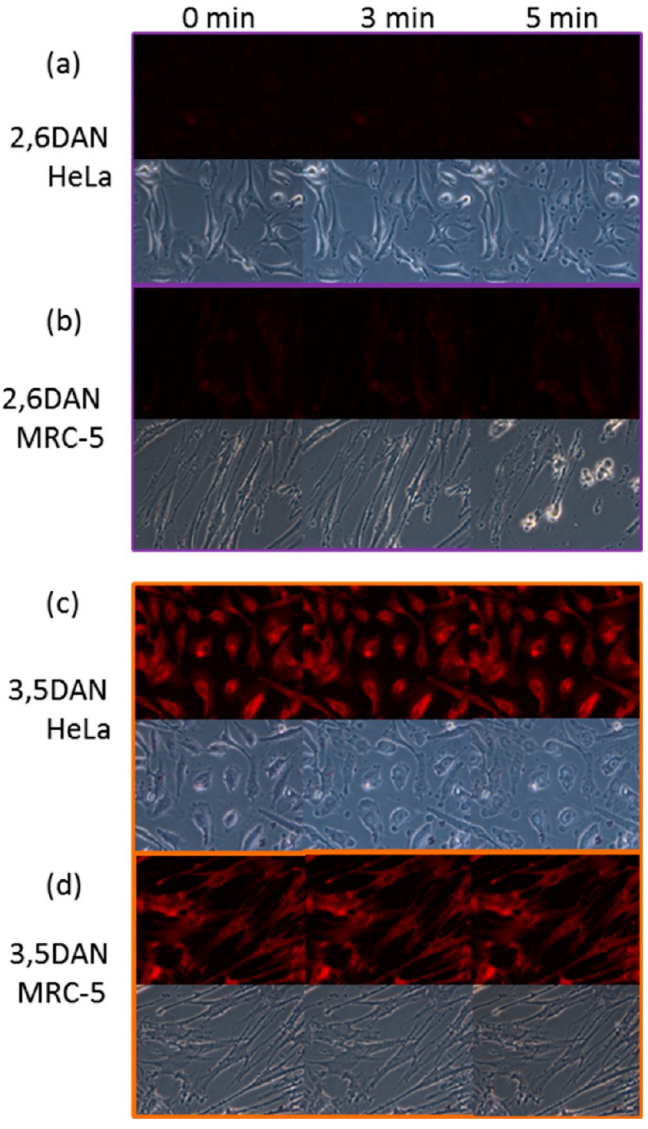

Figure 3. Several selected fluorescent and bright-field photodamage images from a real-time video of (a, c) HeLa cancer cells and (b, d) MRC-5 normal cells incubated with 10 μM 2,6DAN (a, b) or 3,5DAN (c, d) for 12 h followed by irradiating with a 535 ± 25 nm light source from the mercury lamp of the fluorescent microscope.

3.4. Intracellular Accumulation. Following the experimental conditions used in Figure 3, we tried to determine the quantitative accumulation of compounds in the cells using red (590 nm long pass) filters, as shown in Figure S3. Compound 3,5DAN presented clearer concentration-dependent intracellular fluorescent signals because of its higher emission quantum yield, and the intracellular accumulation between cancer cells and normal cells was equivalent. The intracellular accumulation of compound 2,6DAN was difficult to observe because of its low fluorescent quantum yield. Thus, the kinetics of compound uptake was determined by the extraction of the compound from cells.[44] The increase of the compound concentration in the cells was quantified by monitoring the spectral signals of compounds in the ethyl acetate layer after extraction from the cells, as described in the Experimental Section (Figure 4). No apparent difference in the cellular

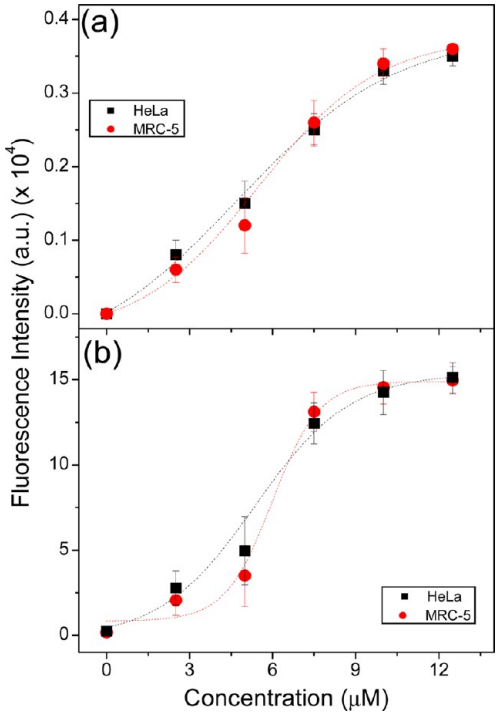

Figure 4. Intracellular accumulation of 2,6DAN (a) and 3,5DAN (b) in MRC-5 normal and HeLa cancer cells, respectively. The cells were incubated with different concentrations of the compounds for 12 h, and the intracellular uptake of the compounds was estimated from a fluorescence calibration curve of the ethyl acetate layer after extraction from the cells. Each data plot represents the average from three separate experiments.

dx.doi.org/10.1021/am403593m | ACS Appl. Mater. Interfaces 2013, 5, 12935−12943

uptake of these two compounds was observed between the cancer cells and normal cells. This notable observation led us to propose that the intracellular uptake of the compound may not be the factor causing selective photodamage, especially in 3,5DAN.

3.5. Subcellular Localization. The intracellular localization of photosensitizers is known to affect strongly the mechanism of cell death. The biological efficacy for most photosensitizers to tumors depends on their abilities to translocate across cellular membranes and on their delivery into specific organelles within cancer cells.[45] To determine subcellular localization, the cells incubated with compound 3,5DAN were double-stained with a green cellular tracker, which merged with the red light emission region of the compound. Figure 5a shows that 3,5DAN was localized

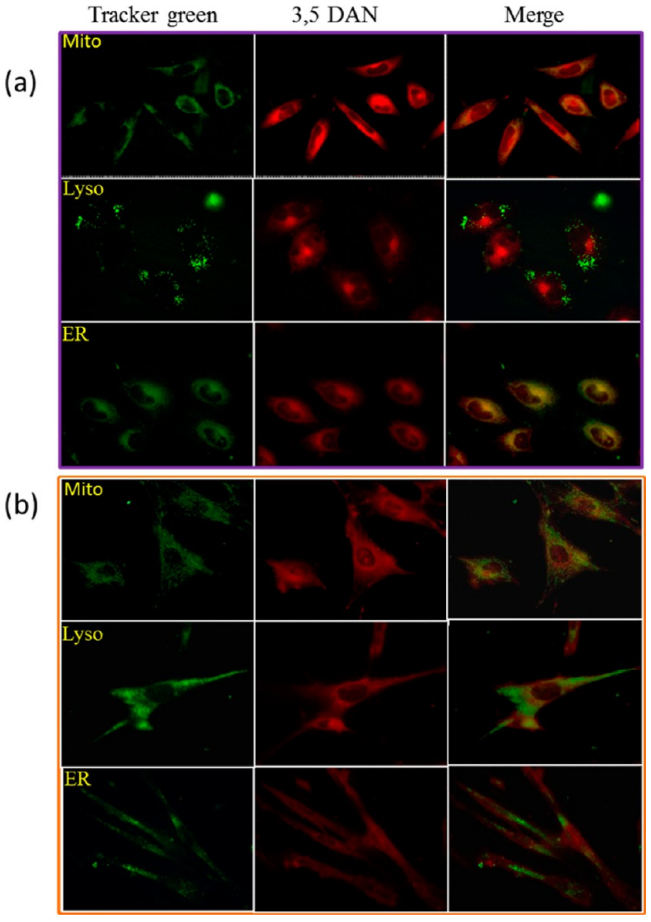

Figure 5. Subcellular localization of 3,5DAN in (a) HeLa cancer cells and (b) MRC-5 normal cells. The images of tracker green were excited by a blue light that was guided through a 470 ± 20 nm bp filter, and the emission wavelength range was collected through a 510 nm lp filter. The red images of the compound were excited by a green light that was guided through a 535 ± 25 nm bp filter, and the emission wavelength range was collected through a 590 nm lp filter.

predominantly in the endoplasmic reticulum (ER) and to a lesser extent in the mitochondria of cancer cells. Alternatively, there was no apparent colocalization between 3,5DAN and these trackers in normal cells (Figure 5b). We inferred that the cellular localization might be the main reason that 3,5DAN can selectively kill cancer cells but not normal cells under suitable irradiation condition. In general, photodamage to mitochondria has been reported to be the primary cause of apoptosis during PDT because the mitochondria play an extremely important role in various cell biological processes, such as apoptotic cell death, molecular metabolism, cell redox status, and energy production.[46,47] However, the ER is also a very attractive site for the localization of photosensitizers to improve the efficiency of PDT. The oxidation of ER proteins because of PDT is known to cause changes in ER Ca^{2+} homeostasis and/or the aggregation of unfolded and misfolded proteins.[48] For example, the ER-localizing photosensitizer Foscan was recently shown to cause Bcl-2 photodamage, possibly specifically affecting the ER pool of Bcl-2 in cancer cells.[37] On the basis of the literature, PDT with photosensitizers that target mitochondria and ER will likely cause photodamage to Bcl-2 and Bcl-xL,[49] and this type of photodamage to these antiapoptotic proteins may cause cell death immediately upon light exposure;[50] the results in Figure 3 seem to confirm this inference.

3.6. Phototoxicity. The combination of compound 3,5DAN and illumination resulted in quantitative cellular toxicity. Figure 6 shows that three different cell lines displayed

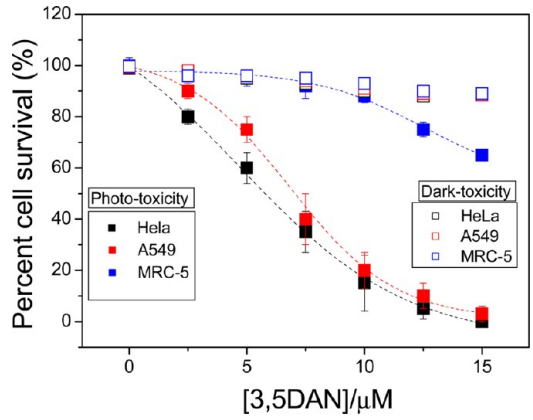

Figure 6. Phototoxicity of HeLa and A549 cancer cells and MRC-5 normal cells treated with different concentrations of 3,5DAN for 12 h before irradiation and after irradiating with a 510 nm lp light source (average 8 J/cm^2); cell death was tested overnight. Each point represents the average from three separate experiments, and the irradiation condition details are described in the Experimental Section.

no observable dark toxicity with 3,5DAN up to a concentration of 15 μM. By contrast, irradiation with an 8 J/cm^2 510 nm long-pass light dose showed apparent phototoxicity, with EC_{50} values for HeLa, A549, and MRC-5 of 4.7, 6.8, and 18.5 μM, respectively. By comparison, the apparent phototoxicity was observed in all cell lines when the system was irradiated with compound 2,6DAN (Figure S4). Additionally, an interesting result was observed when cell death was measured by double-staining cells with Hoechst 33342 and PI.[51] The protocol indicated that the fluorescent color populations (signals) can be separated into three groups: live cells will show only a low level of fluorescence, apoptotic cells will show a higher level of blue fluorescence, and dead cells will show low-blue and high-red fluorescence. Figure 7 shows that in the early stage of cell death (staining with the two probes immediately after illumination), fluorescent images showed an apparent enhancement in blue emission in the nucleus because of the interaction between Hoechst and condensed DNA. Then, the red fluorescence from PI became dominant in the nucleus after the irradiated cell line was cultured overnight. This can be ascribed to the nuclear

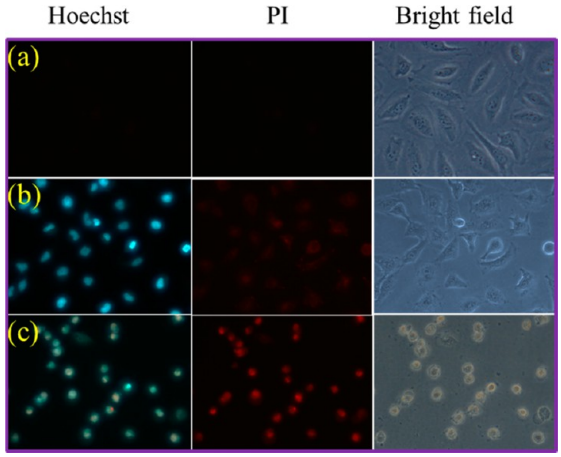

Figure 7. Images of cells following the experimental conditions in Figure 6. (a) Before irradiation (no Hoechst or PI treatment). (b) Cells treated with Hoechst and PI once after irradiation. (c) Cultured cells from panel b after overnight incubation. The images of Hoechst-stained cells were collected by exciting with a blue light that was guided through a 370 ± 10 nm bp filter, and the emission wavelength range was collected through a 450 nm lp filter. The images of PI-stained cells were excited by a green light that was guided through a 530 ± 20 nm bp filter, and the emission wavelength range was collected through a 590 nm lp filter (under these light intensity conditions, the red emission was from PI, not 3,5DAN).

membrane possibly being damaged during a later period of irradiation. This cell death pathway is likely due to an antiapoptosis protein of the mitochondria or ER, as discussed earlier. Furthermore, a comparison of the phototoxicity efficiency of 3,5DAN with those of MB and Foscan (ER-localization photosensitizer) showed a striking imaging result, as illustrated in Figure 8. The phototoxicity efficiency of this

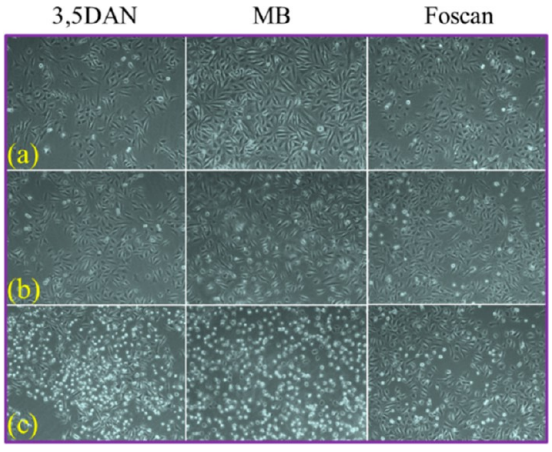

Figure 8. Images of cells following the experimental conditions in Figure 6. Phototoxicity of HeLa cancer cells treated with 10 μM 3,5DAN, methylene (MB), and Foscan for 12 h prior to irradiation. (a) Before irradiation. (b) After irradiation. (c) Cultured cells from panel b after overnight incubation.

compound was better than that of Foscan and nearly equal to that of MB under identical experimental conditions (10 μM incubated reagents, irradiated with a 400−700 nm light source for a more complete comparison), although the singlet oxygen quantum yield of this compound was not as high as those of Foscan and MB. However, we have provided a rare example of a BODIPY derivative as an alternative PDT reagent that presented a selective PDT to cancer cells but not to normal cells.

3.7. New Reactive Oxygen Species Generation. The PDT effects of 3,5DAN were notably more effective than anticipated. Hence, we examined the involvement of other possible mechanisms, such as type I PDT, in the compound's PDT activity. The type I mechanism is usually generated from the interaction of oxygen and free radicals, which involves losing a hydrogen atom or electron-transfer between the excited sensitizer and a substrate to form an active oxygen species, such as the superoxide radical anion.[52,53] Most studies generally suggest that the singlet oxygen formation from type II PDT is primarily responsible for the biological effects of PDT; however, several recent reports illustrate that radical species from the type I mechanism may cause an amplified PDT activity, especially under low-oxygen conditions.[54] The free-radical probe 4-((9-acridinecarbonyl)amino)-2,2,6,6-tetramethylpiperidin-1-oxyl (TEMPO-9-ac, Invitrogen, Carlsbad, CA) captures radicals, resulting in fluorescence ($\lambda_{ex/em}$ = 358/440 nm).[55] Irradiation of 3,5DAN also generates a more apparent increase in signal from TEMPO-9-ac compared to the unchanged levels of the control (Figure 9). This finding indicates that this compound may undergo type I and II PDT simultaneously when it remains in the cells, even though these two types of PDT mechanisms are theoretically competitive pathways.[56]

Furthermore, on the basis of previous studies, subcellular environments (cytosol and organelles) exhibit varying degrees of acidity.[57,45] Once inside a cell, it is likely that the aniline moieties in 3,5DAN, the proton-acceptor functional group, will very probably be protonated. To estimate pK_a values, spectral changes as a function of pH for compound 3,5DAN were measured in H_2O, and their titration fitting curves are shown in Figure S5. The pK_{a1} and pK_{a2} values for the protonated compound are 4.15 and 2.78, respectively. Thus, the ROS properties were rechecked under acidic conditions. Figure 10 illustrates the surprising result that both the singlet oxygen and free-radical yields from the compound increased after irradiation under acidic conditions, especially the singlet oxygen yields. We propose that compound 3,5DAN is not totally protonated in the cell and that the protonation must be dependent on the subcellular localization. However, the ROS generation efficiency of this compound will offer some degree of enhancement once inside the cancer cell. Thus, we conclude that compound 3,5DAN may undergo type I and II PDT simultaneously and that this effect is enhanced by increasing acidity, which makes the PDT efficiency of 3,5DAN much better than that of Foscan and nearly equal to that of MB, especially when the compound remains in the cells.

4. CONCLUSIONS

BODIPY offers many advantageous optical properties. In this study, we successfully used BODIPY derivatives to target cancer cells and demonstrated that 3,5-dianiline-substituted product 3,5DAN may be a potent tumor-specific photosensitizer for PDT. First, we presented an inexpensive and convenient synthesis procedure that can be widely applied to prepare diversified BODIPY derivatives. Second, ROS generation and the biological evolution of cellular uptake, localization, and phototoxicity were determined. The PDT characteristics of the 3,5DAN compound are as follows: it has (1) a selective PDT effect to cancer cells but not normal cells because of the

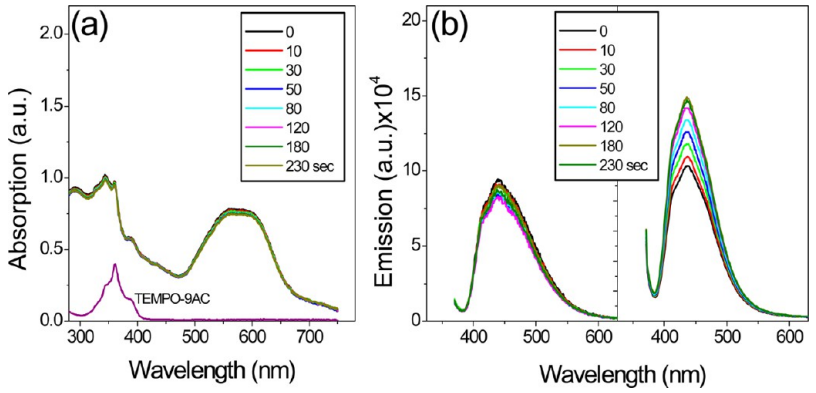

Figure 9. Spectral variability of TEMPO-9ac mixing with compound 3,5DAN upon irradiation following the experimental conditions used in Figure 2. (a) Absorption spectra and (b) emission (λ_{ex} = 360 nm) spectra of TEMPO-9ac upon irradiation without (left) and with compound 3,5DAN (right).

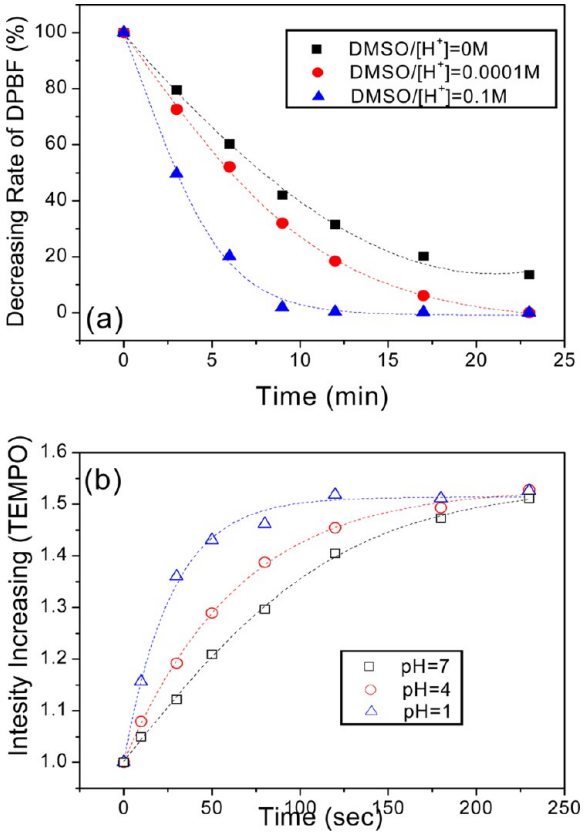

Figure 10. ROS generation assays under acidic conditions. (a) DPBF singlet oxygen (in DMSO) and (b) TEMPO-9ac radical (in aqueous) indicator tests. Experimental conditions follow Figures 2 and 9, respectively.

intracellular localization diversity, (2) a higher photostability than that of methylene blue, (3) a photodamage efficiency that is better than that of Foscan and nearly equal to that of methylene blue, and (4) the support of extra phototoxicity with superoxide generation.

■ ASSOCIATED CONTENT

Ⓢ Supporting Information

Synthesis and characterization data, absorption spectra variations of 20 μM DPBF consumption, concentration-dependent accumulation images of 3,5DAN in cells, photo-toxicity of HeLa and A549 cancer cells and MRC-5 normal cells treated with different concentrations of 2,6DAN, and absoption spectra changes as a function of pH for compound 3,5DAN in H_2O. This material is available free of charge via the Internet at http://pubs.acs.org.

■ AUTHOR INFORMATION

Corresponding Author

*E-mail: ccchang555@dragon.nchu.edu.tw.

Notes

The authors declare no competing financial interest.

■ ACKNOWLEDGMENTS

This work was supported financially by the National Science Council (NSC 101-2113-M-005-016-MY3) of Taiwan.

■ REFERENCES

(1) Lissi, E. A.; Encinas, M. V.; Lemp, E.; Rubio, M. A. *Chem. Rev.* **1993**, *93*, 699−723.
(2) Sternberg, E. D.; Dolphin, D.; Brückner, C. *Tetrahedron* **1998**, *54*, 4151−4202.
(3) Nyman, E. S.; Hynninen, P. H. *J. Photochem. Photobiol., B* **2004**, *73*, 1−28.
(4) Harris, F.; Chatfield, L. K.; Phoenix, D. A. *Curr. Drug Targets* **2005**, *6*, 615−627.
(5) Wainwright, M. *Photodiag. Photodyn. Ther.* **2005**, *2*, 263−272.
(6) Wainwright, M.; Phoenix, D. A.; Rice, L.; Burrow, S. M.; Waring, J. *J. Photochem. Photobiol., B* **1997**, *40*, 233−239.
(7) Uzdensky, A. B.; Iani, V.; Ma, L. W.; Moan. *Photochem. Photobiol.* **2002**, *76*, 320−328.
(8) Sjoback, R.; Nygren, J.; Kubista, M. *Spectrochim. Acta, Part A* **1995**, *51*, L7−L21.
(9) Lovell, J. F.; Liu, T. W.; Chen, J.; Zheng, G. *Chem. Rev.* **2010**, *110*, 2839−2857.
(10) Orenstein, A.; Kostenich, G.; Roitman, L.; Shechtman, Y.; Kopolovic, Y.; Ehrenberg, B.; Malik, Z. *Br. J. Cancer* **1996**, *73*, 937−944.
(11) Kessel, D. *J. Porphyrins Phthalocyanines* **2004**, *8*, 1009−1014.
(12) Tijerina, M.; Kopeckova, P.; Kopecek, J. *Pharm. Res.* **2003**, *20*, 728−737.
(13) Li, G.; Pandey, S. K.; Graham, A.; Dobhal, M. P.; Mehta, R.; Chen, Y.; Gryshuk, A.; Rittenhouse-Olson, K.; Oseroff, A.; Pandey, R. K. *J. Org. Chem.* **2004**, *69*, 158−172.
(14) Hamblin, M. R.; Newman, E. L. *J. Photochem. Photobiol., B* **1994**, *26*, 147−157.
(15) Mestre, B.; Pitie, M.; Loup, C.; Claparols, C.; Pratviel, G.; Meunier, B. *Nucleic Acids Res.* **1997**, *25*, 1022−1027.

(16) Gijsens, A.; Missiaen, L.; Merlevede, W.; de Witte, P. *Cancer Res.* **2000**, *60*, 2197−2202.
(17) Hudson, R.; Carcenac, M.; Smith, K.; Madden, L.; Clarke, O. J.; Pelegrin, A.; Greenman, J.; Boyle, R. W. *Br. J. Cancer* **2005**, *92*, 1442−1449.
(18) Loudet, A.; Burgess, K. *Chem. Rev.* **2007**, *107*, 4891−4932.
(19) Ulrich, G.; Ziessel, R.; Harriman, A. *Angew. Chem., Int. Ed.* **2008**, *47*, 1184−1201.
(20) Mula, S.; Ray, A. K.; Banerjee, M.; Chaudhuri, T.; Dasgupta, K.; Chattopadhyay, S. *J. Org. Chem.* **2008**, *73*, 2146−2154.
(21) Kabayashi, H.; Ogawa, M.; Alford, R.; Choylle, P. L.; Urano, Y. *Chem. Rev.* **2010**, *110*, 2620−2640.
(22) Li, Z.; Bittman, R. *J. Org. Chem.* **2007**, *72*, 8376−8382.
(23) Coskun, A.; Akkaya, E. U. *J. Am. Chem. Soc.* **2005**, *127*, 10464−10465.
(24) Krumova, K.; Oleynik, P.; Karam, P.; Cosa, G. *J. Org. Chem.* **2009**, *74*, 3641−3651.
(25) Hudnall, T. W.; Gabbai, F. P. *Chem. Commun.* **2008**, 4596−4597.
(26) Zeng, L.; Miller, E. W.; Pralle, A.; Isacoff, E. Y.; Chang, C. J. *J. Am. Chem. Soc.* **2006**, *128*, 10−11.
(27) Atilgan, S.; Ozdemir, T.; Akkaya, E. U. *Org. Lett.* **2008**, *10*, 4065−4067.
(28) Ulrich, G.; Goeze, C.; Guardigli, M.; Roda, A.; Ziessel, R. *Angew. Chem., Int. Ed.* **2005**, *44*, 3694−3698.
(29) Li, F.; Yang, S. I.; Ciringh, Y. Z.; Seth, J.; Martin, C. H.; Singh, D. L.; Kim, D.; Birge, R. R.; Bocian, D. F.; Holten, D.; Lindsey, J. L. *J. Am. Chem. Soc.* **1998**, *120*, 10001−10017.
(30) Erten-Ela, S.; Yilmaz, M. D.; Icli, B.; Dede, Y.; Icli, S.; Akkaya, E. U. *Org. Lett.* **2008**, *10*, 3299−3302.
(31) Kamkaew, A.; Lim, S. H.; Lee, H. B.; Kiew, L. V.; Chung, L. Y.; Burgess, K. *Chem. Soc. Rev.* **2013**, *42*, 77−88.
(32) Zhang, X.-F.; Yang, X. *J. Phys. Chem. B* **2013**, *117*, 5533−5539.
(33) Adarsh, N.; Avirah, R. R.; Ramaiah, D. *Org. Lett.* **2010**, *12*, 5720−5723.
(34) Yogo, T.; Urano, Y.; Ishitsuka, Y.; Maniwa, F.; Nagano, T. *J. Am. Chem. Soc.* **2005**, *127*, 12162−12163.
(35) Gorman, A.; Killoran, J.; O'Shea, C.; Kenna, T.; Gallagher, W. M; O'Shea, D. F. *J. Am. Chem. Soc.* **2004**, *126*, 10619−10631.
(36) Lim, S. H.; Thivierge, C.; Nowak-Sliwinska, P.; Han, J.; van den Bergh, H.; Wagnieres, G.; Burgess, K.; Lee, H. B. *J. Med. Chem.* **2010**, *53*, 2865−2874.
(37) Teiten, M. H.; Bezdetnaya, L.; Morlière, P.; Santus, R.; Guillemin, F. *Br. J. Cancer* **2003**, *88*, 146−152.
(38) Chang, C. C.; Hsieh, M. C.; Lin, J. C.; Chang, T. C. *Biomaterials* **2012**, *33*, 897−906.
(39) Velapoldi, R. A.; Tonnesen, H. H. *J. Fluoresc.* **2004**, *14*, 465−472.
(40) Gollnick, K.; Griesbeck, A. *Tetrahedron* **1985**, *41*, 2057−2068.
(41) Zhang, X.-F.; Yang, X. P. *J. Phys. Chem. B* **2013**, *117*, 9050−9055.
(42) Chin, K. K.; Trevithick-Sutton, C. C.; McCallum, J.; Jockusch, S.; Turro, N. J.; Scaiano, J. C.; Foote, C. S.; Garcia-Garibay, M. A. *J. Am. Chem. Soc.* **2008**, *130*, 6912−6913.
(43) Moan, J. *Cancer Lett.* **1986**, *33*, 45−53.
(44) Cheng, Y.; Samia, A. C; Li, J.; Kenney, M. E.; Resnick, A.; Burda, C. *Langmuir* **2010**, *26*, 2248−2255.
(45) Dougherty, T. J.; Gomer, C. J.; Henderson, B. W.; Jori, G.; Kessel, D.; Korbelik, M.; Moan, J.; Peng, Q. J. *J. Natl. Cancer Inst.* **1998**, *90*, 889−905.
(46) Castano, A. P.; Demidova, T. N.; Hamblin, M. R. *Photodiag. Photodyn. Ther.* **2005**, *2*, 1−23.
(47) Rodriguez, M. E.; Azizuddin, K.; Zhang, P.; Chiu, S. M.; Lam, M.; Kenney, M. E.; Burda, C.; Oleinick, N. L. *Mitochondrion* **2008**, *8*, 237−246.
(48) *Advances in Photodynamic Therapy: Basic, Translational, and Clinical*; Hamblin, M. R., Mroz, P., Eds.; Artech House: Boston, MA, 2008; pp 71−74.
(49) Xue, L. Y.; Chiu, S. M.; Oleinick, N. L. *Oncogene* **2001**, *20*, 3420−3427.
(50) Kessel, D.; Arroyo, A. S. *Photochem. Photobiol. Sci.* **2007**, *6*, 1290−1295.
(51) Belloc, F.; Dumain, P.; Boisseau, M. R.; Jalloustre, C.; Reiffers, J.; Bernard, P.; Lacombe, F. *Cytometry* **1994**, *17*, 59−65.
(52) DeRosa, M. C.; Crutchley, R. J. *Coord. Chem. Rev.* **2002**, *233−234*, 351−371.
(53) Castano, A. P.; Mroz, P.; Hamblin, M. R. *Nat. Rev. Cancer* **2006**, *6*, 535−545.
(54) Silva, E. F. F.; Serpa, C.; Dabrowski, J. M.; Monteiro, C. J. P.; Formosinho, S. J.; Stochel, G.; Urbanska, K.; Simoes, S.; Pereira, M. M.; Arnaut, L. G. *Chem.—Eur. J.* **2010**, *16*, 9273−9286.
(55) Bulina, M. E.; Chudakov, D. M.; Britanova, O. V.; Yanushevich, Y. G.; Staroverov, D. B.; Chepurnykh, T. V.; Merzlyak, E. M.; Shkrob, M. A.; Lukyanov, S.; Lukyanov, K. A. *Nat. Biotechnol.* **2006**, *24*, 95−99.
(56) Dougherty, T. J.; Gomer, C. J.; Henderson, B. W.; Jori, G.; Kessel, D.; Korbelik, M.; Moan, J.; Peng, Q. J. *J. Natl. Cancer Inst.* **1998**, *90*, 889−905.
(57) Lin, H. H.; Su, S. Y.; Chang, C. C. *Org. Biomol. Chem.* **2009**, *7*, 2036−2039.